

Magnetic properties of the itinerant metamagnetic system $\text{Co}(\text{S}_{1-x}\text{Se}_x)_2$ under high magnetic fields and high pressure

T. Goto,* Y. Shindo, and H. Takahashi

Institute for Solid State Physics, University of Tokyo, Roppongi, Minato-ku, Tokyo 106, Japan

S. Ogawa

Faculty of Engineering, Tokyo Denki University, Kanda, Chiyoda-ku, Tokyo 101, Japan

(Received 20 February 1997)

The magnetization of the $\text{Co}(\text{S}_{1-x}\text{Se}_x)_2$ system with $0 \leq x \leq 0.2$ has been measured under high magnetic fields and high pressure. Ferromagnetic CoS_2 exhibits a second-order transition at $T_c = 122$ K. Substitution of 10% Se for S in CoS_2 reduces the Curie temperature to $T_c = 27$ K and the transition to first order. $\text{Co}(\text{S}_{1-x}\text{Se}_x)_2$ with $0.12 \leq x$ becomes an exchange-enhanced Pauli paramagnet. The itinerant metamagnetic transition has been observed in the paramagnet. $\text{Co}(\text{S}_{0.9}\text{Se}_{0.1})_2$ also shows a transition just above T_c . Using the experimental data, the magnetic phase diagram of $\text{Co}(\text{S}_{1-x}\text{Se}_x)_2$ is determined. With increasing pressure, the Curie temperature of CoS_2 decreases and the ferromagnetic transition changes to first order at $P \approx 0.4$ GPa. In the pressure regime of the first-order transition $P > 0.4$ GPa, the metamagnetic transition is observed just above T_c . In $\text{Co}(\text{S}_{0.9}\text{Se}_{0.1})_2$, the ferromagnetism disappears at 0.25 GPa and paramagnetism appears. The observed magnetic properties and the magnetic phase diagram of $\text{Co}(\text{S}_{1-x}\text{Se}_x)_2$ can be qualitatively described with a theory of the itinerant electron metamagnetism at finite temperatures. [S0163-1829(97)06045-1]

I. INTRODUCTION

Since itinerant electron metamagnetism, that is, the first-order field-induced transition from the paramagnetic to the ferromagnetic state in the itinerant electron system, was predicted to occur in a paramagnetic metal with a suitable energy dependence of the density-of-states (DOS) curve around the Fermi level,¹ many theoretical²⁻⁵ and experimental⁶⁻¹¹ studies have been made to elucidate it. Our group systematically studied the magnetization processes of various Co-based pseudobinary compounds such as $\text{Y}(\text{Co}_{1-x}\text{Al}_x)_2$,¹² $\text{Lu}(\text{Co}_{1-x}\text{Al}_x)_2$,¹³ $\text{Hf}(\text{Co}_{1-x}\text{Fe}_x)_2$,¹⁴ and $\text{Lu}(\text{Co}_{1-x}\text{Ga}_x)_2$ (Ref. 15) in magnetic fields up to 120 T and clearly observed the itinerant metamagnetic transitions in these compounds. On the other hand, Adachi *et al.* found the metamagnetic transitions in the paramagnetic $\text{Co}(\text{S}_{1-x}\text{Se}_x)_2$ compounds.^{16,17}

We found that every metamagnetic compound has characteristics of a nearly ferromagnetic metal.¹¹ The electronic specific heat and magnetic susceptibility of the compound are very large and the temperature dependence of the susceptibility is anomalous: the susceptibility increases and then decreases through a maximum value. This indicates that the anomalous behavior of the susceptibility also originates from the shape of the DOS curve. It should be noted that the observed metamagnetic transitions appear with low critical fields in the above paramagnetic pseudobinary systems that are very close to their ferromagnetic instabilities and that the critical field increases as the composition of the systems goes away from the ferromagnetic region. This suggests that the mechanism of the appearance of the metamagnetic transition is closely related to that of the ferromagnetic instability.

The $\text{Co}(\text{S}_{1-x}\text{Se}_x)_2$ system has the pyrite structure.¹⁸ This structure is cubic and can be considered as an NaCl-like

structure consisting of Co atoms and chalcogen atom pairs. It has been known from the electrical, magnetic, optical, and x-ray photoemission spectroscopy experiments¹⁹⁻²¹ that the 3d electrons arising from the Co atoms are in the low-spin state. The 3d band is split into t_{2g} and e_g subbands by a crystalline field. The t_{2g} band is completely filled with 3d electrons. On the other hand, the e_g band is partially filled with one 3d electron per Co atom. Therefore, the 3d electrons in the e_g band are responsible for the magnetic properties. The e_g states are hybridized with the antibonding p^* states arising from the chalcogen atom pairs.²² The hybridization between the e_g and p^* states in CoSe_2 is stronger than that in CoS_2 . In fact, recent band-structure calculations of CoS_2 and CoSe_2 indicate that the latter e_g band is wider than the former one and the structures of both e_g bands are very similar to each other.²³ Therefore, the increase of the Se concentration in $\text{Co}(\text{S}_{1-x}\text{Se}_x)_2$ makes the bandwidth wider. CoS_2 is an itinerant ferromagnet with a Curie temperature of $T_c = 122$ K.^{16,18} The Curie temperature is rapidly decreased by the substitution of Se for S in CoS_2 .^{16,18} The ferromagnetic compound with $x = 0.05$ and 0.1 near the disappearance of ferromagnetism seems to show a first-order transition at the Curie temperature.¹⁸ $\text{Co}(\text{S}_{1-x}\text{Se}_x)_2$ with $x \geq 0.12$ becomes an exchange-enhanced Pauli paramagnet in which the metamagnetic transition is induced by the application of high magnetic fields.^{16,17} These results indicate that the $\text{Co}(\text{S}_{1-x}\text{Se}_x)_2$ system is one of the most suitable systems for studying the relation between the ferromagnetic instability and the appearance of the metamagnetic transition observed in the itinerant metamagnetic systems.

The application of high pressure can finely increase the bandwidth compared with the Se substitution. Thus, high pressure is very useful for examining the detailed variations of the magnetic properties due to the increase of the band-

width. In this study, we have systematically studied the magnetization of the $\text{Co}(\text{S}_{1-x}\text{Se}_x)_2$ system under high magnetic fields and high pressure. Moriya²⁴ and Yamada²⁵ developed a theory of the itinerant electron metamagnetism at finite temperatures based on the spin-fluctuation model. Our experimental results are discussed with this theory.

II. EXPERIMENTAL PROCEDURE

Polycrystalline samples of CoS_2 , CoSe_2 , and their mixed crystals have been prepared by a direct reaction of the constituent elements in a vacuum at elevated temperature.¹⁸ We also followed this method to prepare samples of $\text{Co}(\text{S}_{1-x}\text{Se}_x)_2$ with $0 \leq x \leq 0.3$. We know from previous experiments that the field and the temperature dependence of the magnetization of a metamagnetic sample in the range $0.1 \leq x \leq 0.2$ are extremely sensitive to the local arrangement of S and Se atoms around the Co atom.^{26,27} Since we aimed to obtain the precise magnetization data of $\text{Co}(\text{S}_{1-x}\text{Se}_x)_2$ to compare quantitatively their transition temperatures and critical fields with the theory, we needed to have very good homogeneous samples. In several trials of sample preparation, we found a small amount of selenium segregation and condensations separately in an evacuated quartz tube when the reaction temperature was high, above about 650 °C. This suggests a deficiency in Se or a possible precipitation of microcrystals of a Co-rich phase. On the other hand, the reaction at a temperature below about 650 °C resulted in an incomplete homogeneity of S and Se distribution, which gives extremely broad ferromagnetic and metamagnetic transitions. We prepared the samples used in this study with the following procedure. Cobalt metal of 99.9+ % purity in a powdered form of about 50 μm size, sulfur lump of 99.999% purity and selenium in a shot form of 99.999% purity were mixed in stoichiometric proportions for a desired x value and sealed in a quartz tube at a pressure less than 10^{-4} Torr. The total sample weight was about 4 g. As a preliminary reaction, the sealed tube was heated in an electric furnace for two days at 400 °C, two days at 450 °C, two days at 500 °C, and two days at 550 °C and cooled in the furnace. After removal from the tube, the sample was crushed into fine powder. The powder was vacuum sealed again in a quartz tube and heated for two days at 700 °C, four days at 750 °C, three days at 700 °C, three days at 600 °C, and three days at 500 °C and cooled. The samples prepared as above were powdered for magnetization measurements.

High magnetic fields up to 40 T were produced using a wire-wound pulse magnet with a rise time of about 5 ms. The sample magnetizations in pulsed high magnetic fields were measured using a conventional induction method in the temperature range between 4.2 and 200 K.

Magnetization measurements under high pressure and high magnetic fields are very rare in spite of their importance for magnetic studies. Recently, we made a magnetometer for measuring precisely the magnetizations of weakly magnetic materials under these conditions. We use an extraction method with a nonmagnetic pressure clamp to detect sample magnetizations in high magnetic fields up to 11 T produced by a superconducting magnet. In order to reduce the magnetization background from the clamp, a high-purity TiCu alloy including about 3 wt % Ti is employed as a material of the

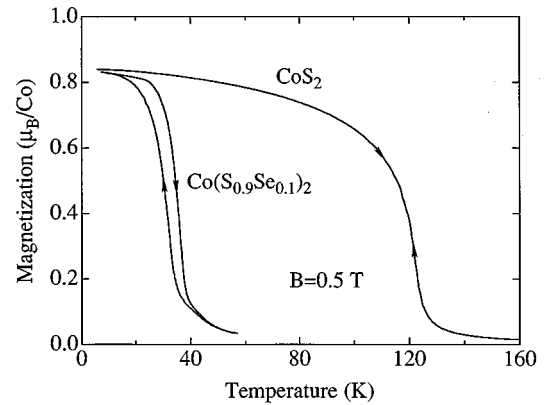


FIG. 1. Temperature variations of the magnetizations of CoS_2 and $\text{Co}(\text{S}_{0.9}\text{Se}_{0.1})_2$ measured in a magnetic field 0.5 T.

locking screws and the clamp cylinder. Because the paramagnetic susceptibility of a small amount of Ti almost compensates the diamagnetic susceptibility of Cu, the susceptibility of this alloy is extremely small, $+3 \times 10^{-9}$ emu/g at room temperature and $+5 \times 10^{-8}$ emu/g at 1.8 K. The increase of the susceptibility at 1.8 K comes from some magnetic impurities. The strength of this material is nearly the same as that of ordinary commercial BeCu containing ferromagnetic Co. The piston caps and pistons are made of high-purity zirconia which shows diamagnetism with a susceptibility -1.7×10^{-7} emu/g. The sample is compressed in a Teflon cell filled with a liquid pressure medium, Fluorinert, in the clamp cylinder. The produced pressure at low temperatures is calibrated by means of the Meissner effect of Pb for which the pressure dependence of the superconducting transition temperature is known to be highly accurate.²⁸ The high pressure clamp has been used for various magnetic studies up to 1.3 GPa. In this pressure range, the plastic deformation inside the clamp is found to be negligibly small. In this study, we measured the magnetizations of CoS_2 and $\text{Co}(\text{S}_{0.9}\text{Se}_{0.1})_2$ under high pressure up to 0.8 GPa and high magnetic field up to 9 T.

III. EXPERIMENTAL RESULTS

A. Magnetizations and susceptibilities

First we show in Fig. 1 the temperature dependence of the magnetization of CoS_2 and $\text{Co}(\text{S}_{0.9}\text{Se}_{0.1})_2$ measured in a magnetic field of 0.5 T. CoS_2 is a ferromagnet with a Curie temperature $T_c = 122$ K. The magnetization decreases more rapidly in the vicinity of the Curie temperature than usual ferromagnets, but the ferromagnetic transition is second order. The magnetization does not depend on the cooling process of the sample. In the case of $\text{Co}(\text{S}_{0.9}\text{Se}_{0.1})_2$, however, the magnetization exhibits hysteresis around the Curie temperature of about 30 K. This indicates that the substitution of 10% Se for S in CoS_2 abruptly decreases the Curie temperature from 122 K to about 30 K and changes the type of the ferromagnetic transition from the second order to the first-order one. In the concentration region $x \geq 0.12$, the $\text{Co}(\text{S}_{1-x}\text{Se}_x)_2$ system becomes paramagnetic.^{16,18}

The temperature dependence of the susceptibility of $\text{Co}(\text{S}_{1-x}\text{Se}_x)_2$ with $x = 0.1-0.3$ is shown in Fig. 2. The susceptibility was measured in a magnetic field, 0.5 T. In the

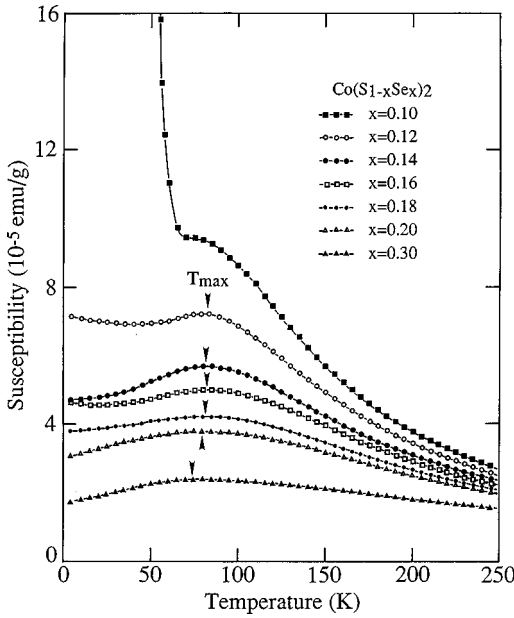


FIG. 2. Temperature variations of the susceptibilities of the $\text{Co}(\text{S}_{1-x}\text{Se}_x)_2$ compounds with $0.1 \leq x \leq 0.3$.

low-temperature region below 50 K, however, the susceptibility is found to be increased by some ferromagnetic impurities included in the sample. In order to eliminate the effect of impurities as much as possible, we have determined the susceptibility in this region from the slope of the magnetization curve after the magnetization of the impurities saturated. The inhomogeneous effect of the pseudobinary sample also increases the susceptibility at low temperatures, especially in the sample near the disappearance of ferromagnetism. Therefore, the value of the susceptibility at low temperatures is less reliable than that at high temperatures, $T > 50$ K. A sharp upturn of the susceptibility observed for $x = 0.1$ originates from the appearance of the ferromagnetic state. All the paramagnetic samples with more than 12% Se exhibit characteristics of nearly ferromagnetic metals: the susceptibilities have a broad maximum around 80 K. The maximum has not been observed clearly in $\text{Co}(\text{S}_{1-x}\text{Se}_x)_2$.^{16,18} The susceptibility of ferromagnetic $\text{Co}(\text{S}_{0.9}\text{Se}_{0.1})_2$ seems to exhibit a broad maximum just above the Curie temperature. Here we define T_{max} as the temperature at which the susceptibility becomes maximum. The susceptibility at T_{max} rapidly increases with decreasing the concentration x .

B. Magnetizations in pulsed high magnetic fields

In order to examine the magnetic properties of the ground states of the $\text{Co}(\text{S}_{1-x}\text{Se}_x)_2$ compounds, we measured the magnetization curves for 4.2 K in pulsed high magnetic fields up to 32 T. The results for $x = 0 - 0.2$ are shown in Fig. 3. All the paramagnetic compounds with $x \geq 0.12$ exhibit the very sharp itinerant metamagnetic transitions to the ferromagnetic state compared with those observed by Adachi *et al.*¹⁷ This suggests that the quality of the present samples are very high. The average critical field of the transitions in ascending and descending fields, B_c , increases linearly with x . The saturation magnetization above B_c decreases slightly

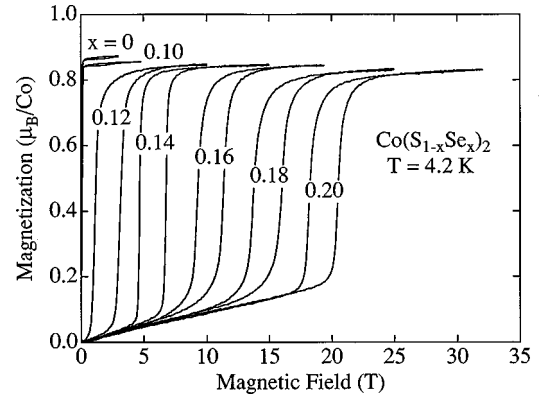


FIG. 3. Magnetization curves of the $\text{Co}(\text{S}_{1-x}\text{Se}_x)_2$ compounds with $0 \leq x \leq 0.2$ measured at 4.2 K in pulsed high magnetic fields up to 32 T.

with increasing x . This value is consistent with the saturation magnetizations of the ferromagnetic compounds with $x = 0$ and 0.1.

We also measured the magnetization curves of all the samples at various temperatures in pulsed high magnetic fields up to 40 T. Figure 4 shows the magnetization curves of ferromagnetic $\text{Co}(\text{S}_{0.9}\text{Se}_{0.1})_2$ at several temperatures between 4.2 and 100 K. This compound, whose ferromagnetic transition is first order, exhibits anomalous magnetic behavior in the paramagnetic temperature region. We can see the relatively sharp metamagnetic transition with hysteresis just above the Curie temperature. With increasing temperature, the first-order transition becomes broad accompanied with the increase of the critical field and finally disappears. It should be noted that CoS_2 with the second-order ferromagnetic transition has no metamagnetic transition in the paramagnetic temperature region.

Figure 5 shows the magnetization curves of paramagnetic $\text{Co}(\text{S}_{0.86}\text{Se}_{0.14})_2$ and $\text{Co}(\text{S}_{0.8}\text{Se}_{0.2})_2$ in the temperature region from 4.2 to 140 K. The observed metamagnetic transition is very sharp at low temperatures. With increasing temperature, however, the transition becomes broad with the increase of the critical field and finally disappears. This behavior is very similar to that of ferromagnetic $\text{Co}(\text{S}_{0.9}\text{Se}_{0.1})_2$ in the paramagnetic temperature region.

The average critical fields of $\text{Co}(\text{S}_{1-x}\text{Se}_x)_2$ with $x = 0.1 - 0.2$ are summarized in Fig. 6(a) as a function of the

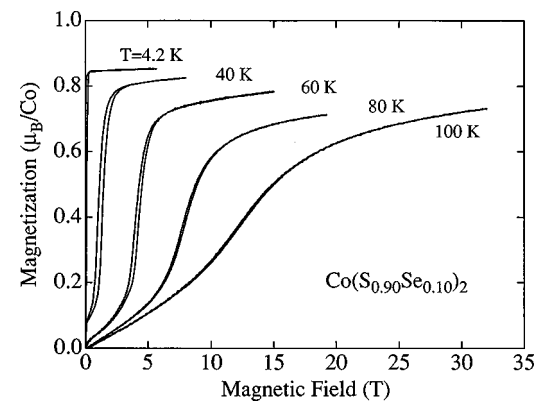


FIG. 4. Magnetization curves of $\text{Co}(\text{S}_{0.9}\text{Se}_{0.1})_2$ at several temperatures.

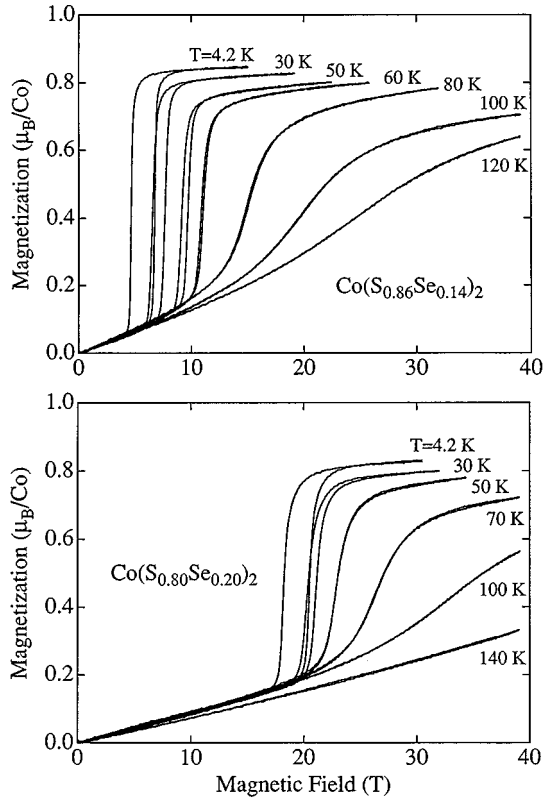


FIG. 5. Magnetization curves of $\text{Co}(\text{S}_{0.86}\text{Se}_{0.14})_2$ and $\text{Co}(\text{S}_{0.80}\text{Se}_{0.20})_2$ at several temperatures.

square of temperature. The critical field shifts proportionally to T^2 and can be written in the low-temperature region $T < 70$ K as

$$B_c(x, T) = B_c(x, 0) + \alpha T^2. \quad (1)$$

Here $B_c(x, 0)$ is the average critical field at $T=0$ K and α is constant. The T^2 dependence has already been found in paramagnetic Co-based Laves phase compounds.^{11–13,29} The ferromagnetic compound with $x=0.1$ and the paramagnetic ones with $x \geq 0.12$ have the same value of α (>0). The value of $B_c(x, T)$ for ferromagnetic $\text{Co}(\text{S}_{0.9}\text{Se}_{0.1})_2$ should become zero at the Curie temperature: $B_c(0.1, T_c) = 0$. From this relation, we can correctly determine the equilibrium value of T_c to be 27 K. Figure 6(b) shows the estimated average critical field at $T=0$ K as a function of x . The critical field increases linearly with x . The critical concentration x_c at which the transition field becomes zero corresponds to the disappearance of ferromagnetism. The critical concentration is estimated to be $x_c = 0.11$.

The critical temperature T_0 for the disappearance of the metamagnetic transition can be determined from the temperature at which the hysteresis of the magnetization curve disappears. As an example, Fig. 7 shows the difference between the critical fields in increasing and decreasing fields in the sample with $x=0.14$. The difference ΔB_c decreases nearly linearly with temperature and becomes zero at T_0 .

Using the observed values of the Curie and critical temperatures T_c and T_0 , we have determined the magnetic phase diagram of $\text{Co}(\text{S}_{1-x}\text{Se}_x)_2$ in the x - T plane, which is shown in Fig. 8. The ferromagnetic transition is second order at x

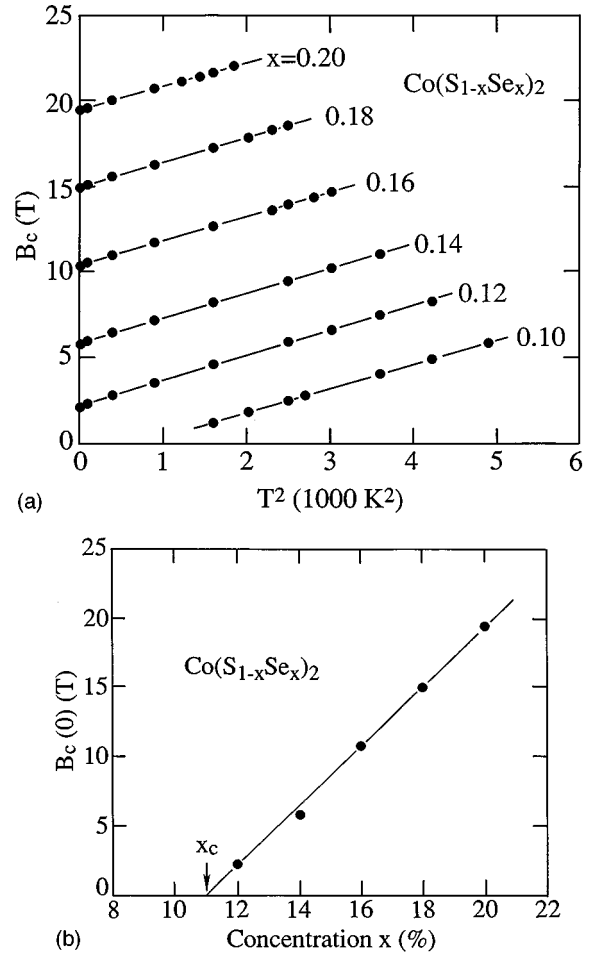


FIG. 6. (a) Average critical fields of the $\text{Co}(\text{S}_{1-x}\text{Se}_x)_2$ compounds with $0.1 \leq x \leq 0.2$, B_c , as a function of the square of the temperature. (b) Estimated average critical fields at $T=0$ K, $B_c(0)$, as a function of the concentration x .

$=0$, but becomes first order at $x=5$ and 10%.¹⁶ The value of T_c on the first-order phase boundary abruptly decreases with increasing x . As described in discussion, the position of T_t on the T_c line where the type of the ferromagnetic transition

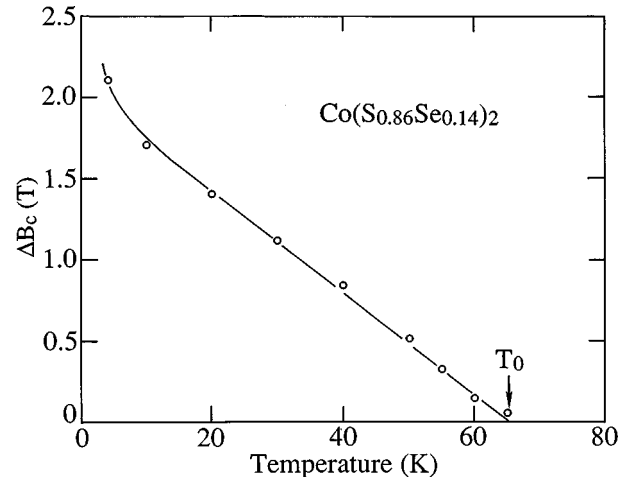


FIG. 7. Difference between the critical fields ΔB_c of $\text{Co}(\text{S}_{0.86}\text{Se}_{0.14})_2$ observed in increasing and decreasing fields. At a temperature T_0 , the metamagnetic transition disappears.

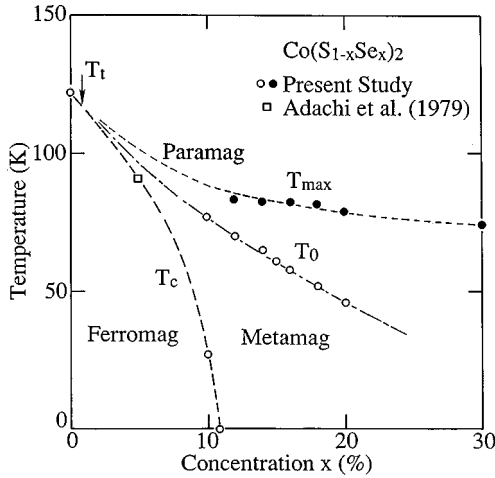


FIG. 8. Magnetic phase diagram of $\text{Co}(\text{S}_{1-x}\text{Se}_x)_2$ in the x - T plane. Below the T_c line, ferromagnetism appears. With increasing x , the type of the ferromagnetic transition is expected to change at the point T_t on the T_c line, which corresponds to a concentration $x = 1\%$. Between the T_c and T_0 lines, the metamagnetic transition occurs. The values of T_{\max} are also plotted, at which the susceptibility becomes maximum.

changes from the second order to the first-order one can be determined from the critical concentration x_t at which $\chi(T_{\max})^{-1} = 0$ is satisfied.²⁵ The estimated critical concentration is $x_t = 1\%$. Therefore, the second-order transition region exists only in the vicinity of $x = 0$. In the concentration region $1\% < x < 11\%$, however, the transition becomes first order. The T_0 line, on which the metamagnetic transition disappears, is expected to merge into the T_c line at T_t .²⁵ Between the T_c and T_0 lines, the metamagnetic transition appears as shown in Fig. 8. For comparison, the values of T_{\max} are also plotted in the x - T plane. The observed value of T_{\max} is larger than that of T_0 at the same concentration x . The T_{\max} line is also expected to merge into the T_c line at T_t .²⁵

C. Magnetizations under static high field and high pressure

We measured the magnetizations of ferromagnetic CoS_2 and $\text{Co}(\text{S}_{0.9}\text{Se}_{0.1})_2$ under static high magnetic field and high pressure. Figure 9(a) shows the temperature dependence of the magnetization of CoS_2 in a magnetic field of 0.5 T at various pressures. The magnetization was measured with increasing temperature after zero-field cooling of the sample. In the low-temperature region, the pressure effect on the magnetization is small. In the vicinity of the Curie temperature, however, this effect is very large. In order to examine in detail the magnetic behavior of CoS_2 under high pressure around the Curie temperature, we measured again the magnetization in a magnetic field of 0.1 T at various pressures. Figure 9(b) shows the magnetization around the Curie temperature. With increasing pressure, the magnetization decreases more abruptly at the Curie temperature. This indicates that the second-order ferromagnetic transition is changed into the first-order one by the application of high pressure $P > 0.4$ GPa.

At ambient pressure, CoS_2 has no metamagnetic transition above the Curie temperature. Under high pressure where the

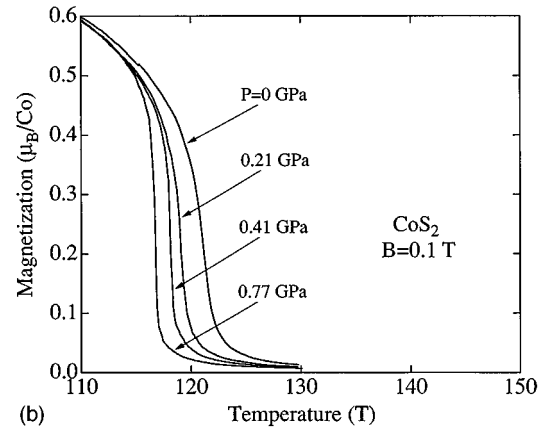
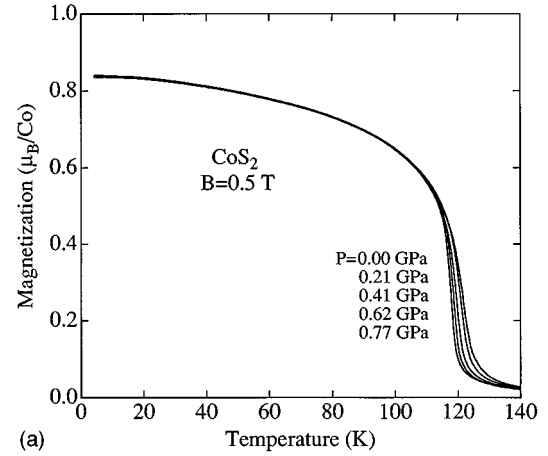


FIG. 9. (a) Temperature dependence of the magnetization of CoS_2 measured in a magnetic field of 0.5 T at several pressures. (b) Magnetization of CoS_2 around the Curie temperature measured in a magnetic field of 0.1 T.

ferromagnetic transition becomes first order, we have observed the metamagnetic transition just above the Curie temperature. As a typical example, we show the temperature dependence of the magnetization curve of CoS_2 at 0.77 GPa in Fig. 10. As shown in the inset, the magnetization curve for 117 K clearly indicates the metamagnetic transition with hysteresis. It should be noted that $\text{Co}(\text{S}_{0.9}\text{Se}_{0.1})_2$ with the

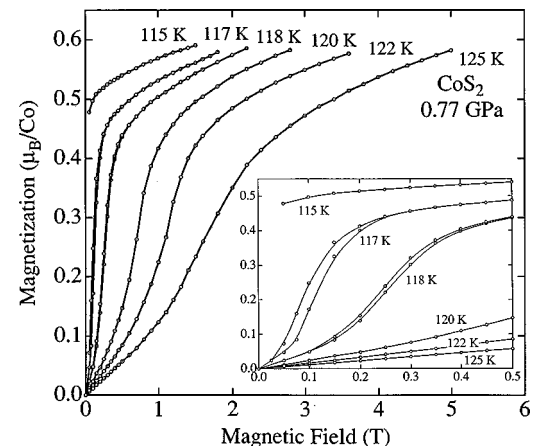


FIG. 10. The magnetization curves of CoS_2 for 0.77 GPa around the Curie temperature. The inset shows the magnetization curves on a finer magnetic field scale.

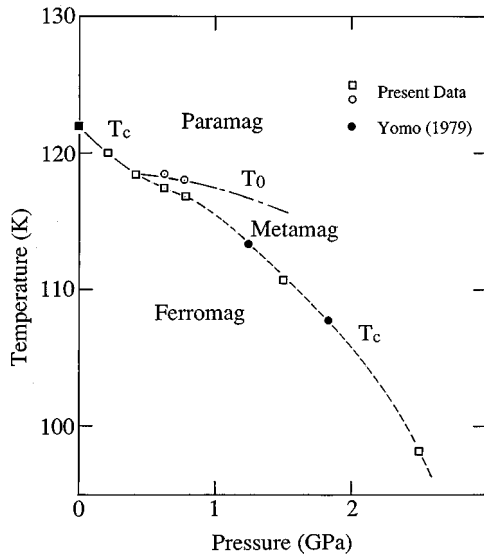


FIG. 11. Magnetic phase diagram of CoS_2 in the P - T plane. The Curie temperature T_c above 1 GPa has been determined from the ac susceptibility measurements. Yomo's data (Ref. 30) of T_c are also plotted for comparison. The ferromagnetic transition is second order below $P \approx 0.4$ GPa and first order above this pressure. Between the T_c and T_0 lines, the metamagnetic transition appears.

first-order ferromagnetic transition at ambient pressure also exhibits the metamagnetic transition above T_c (see Fig. 4).

Figure 11 shows the magnetic phase diagram of CoS_2 in the P - T plane. The Curie temperature has been determined from the magnetization measurements in the pressure region $P \leq 0.77$ GPa and from the ac susceptibility measurements above this region. The data of Yomo³⁰ are also plotted for comparison. It should be noted that the change of T_c around 0.4 GPa is anomalous: T_c decreases linearly with increasing pressure in the low-pressure region $0 \leq P \leq 0.41$ GPa, but above 0.41 GPa it deviates remarkably from this linear relation. Above 1 GPa, T_c decreases more rapidly. The values of T_0 at $P = 0.62$ and 0.77 GPa are very close to that of T_c for $P = 0.41$ GPa. We have observed the metamagnetic transition in the narrow temperature region between T_0 and T_c lines.

$\text{Co}(\text{S}_{0.9}\text{Se}_{0.1})_2$ is a ferromagnet near the disappearance of ferromagnetism and its pressure effect is expected to be very large. In order to examine the change of the magnetic ground state by the application of high pressure, we measured the magnetization curves for 4.2 K at several pressures. The results are shown in Fig. 12. With increasing pressure, the spontaneous magnetization abruptly decreases and the ferromagnetic compound becomes paramagnetic under pressures higher than 0.21 GPa. In the paramagnetic pressure region, the metamagnetic transition occurs. The magnetization after the transition is nearly equal to the saturation magnetization at $P = 0$ GPa in the pressure region $0 \leq P \leq 0.77$ GPa.

We measured the temperature dependence of the magnetization curve of $\text{Co}(\text{S}_{0.9}\text{Se}_{0.1})_2$ at various pressures. Figure 13 shows the results for $P = 0.21$ and 0.77 GPa. The critical field increases with increasing pressure and temperature. The metamagnetic transition becomes broad with increasing temperature. Comparing these results with the temperature dependencies of the magnetization curves of $\text{Co}(\text{S}_{1-x}\text{Se}_x)_2$ for various concentration, we conclude that the change of the

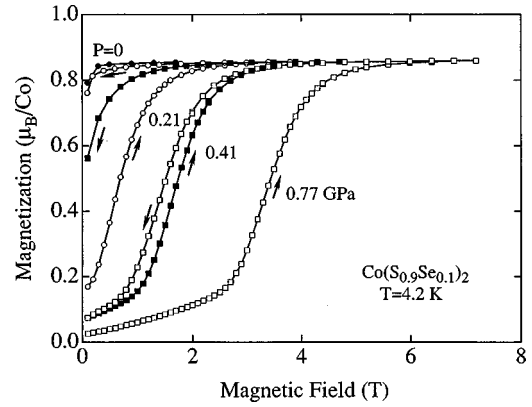


FIG. 12. Pressure dependence of the magnetization curve of $\text{Co}(\text{S}_{0.9}\text{Se}_{0.1})_2$ at $T = 4.2$ K.

magnetic properties by the application of high pressure is almost the same as that due to the Se substitution (see Figs. 4 and 5).

The average critical fields of $\text{Co}(\text{S}_{0.9}\text{Se}_{0.1})_2$ at various pressures are summarized in Fig. 14(a) as a function of the square of temperature. The transition field under high pressure also shifts proportionally to T^2 at low temperatures and can be written by

$$B_c(P, T) = B_c(P, 0) + \alpha T^2. \quad (2)$$

Here $B_c(P, 0)$ is the average critical field for $P = 0$ GPa. In the pressure region $0 \leq P \leq 0.77$ GPa, α (> 0) is constant and its value is equal to that of α in Eq. (1). From both Eqs. (1) and (2), we consider that the value of α for $\text{Co}(\text{S}_{1-x}\text{Se}_x)_2$ does not change in the pressure and concentration regions

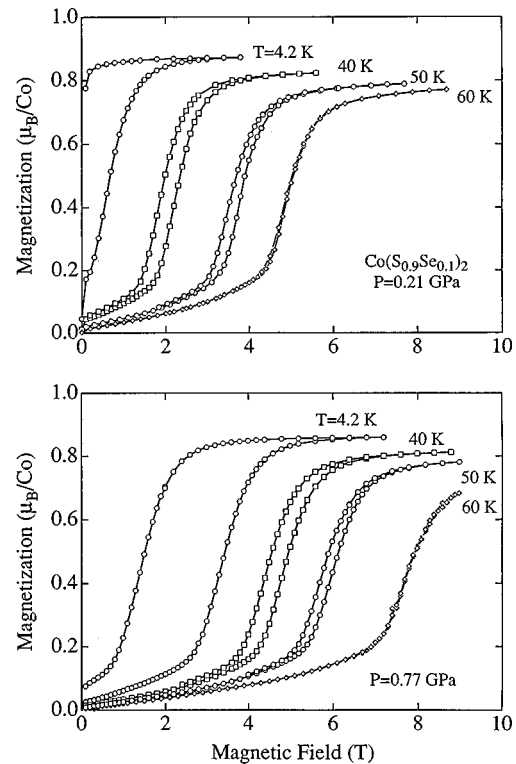


FIG. 13. Temperature dependence of the magnetization curve of $\text{Co}(\text{S}_{0.9}\text{Se}_{0.1})_2$ measured at $P = 0.21$ and 0.77 GPa.

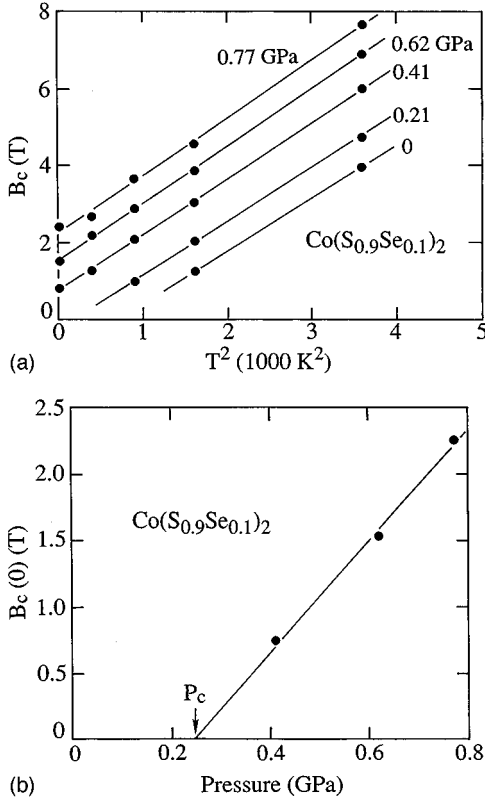


FIG. 14. (a) Average critical fields of $\text{Co}(\text{S}_{0.9}\text{Se}_{0.1})_2$, B_c , for various pressures as a function of the square of temperature. (b) Estimated average critical field for $T=0$ K, $B_c(0)$, as a function of pressure. The critical pressure for the disappearance of ferromagnetism is evaluated to be $P_c=0.25$ GPa.

$0 \leq P \leq 0.77$ GPa and $0.1 \leq x \leq 0.2$ [see Fig. 6(a)]. Figure 14(b) shows the estimated average critical field for $T=0$ K, $B_c(P,0)$, as a function of pressure. The critical field increases linearly with pressure. The critical pressure P_c at which the transition field becomes zero is estimated to be $P_c=0.25$ GPa. This pressure corresponds to the disappearance of ferromagnetism.

IV. DISCUSSION

A. Phase diagram and magnetic properties in high magnetic fields

Moriya²⁴ and Yamada²⁵ have proposed a theory of the itinerant metamagnetic transition at finite temperatures based on the spin-fluctuation model. Here, we abbreviate this theory as the MY theory. In order to use this theory for analyzing our experimental results, we briefly introduce it. The equation of state for an itinerant electron system is written in the ground state as

$$B = aM + bM^3 + cM^5, \quad (3)$$

where B is magnetic field, M the uniform magnetization, and a is the inverse susceptibility at $T=0$ K, $a = \chi(0)^{-1}$. The coefficients a , b , and c are functions of the electronic density of states and its derivatives at the Fermi level. Here M and χ are expressed in terms of μ_B/Co ($=\mu_B/\text{f.u.}$) and μ_B/CoT , respectively. The coefficients a , b , and c for ac-

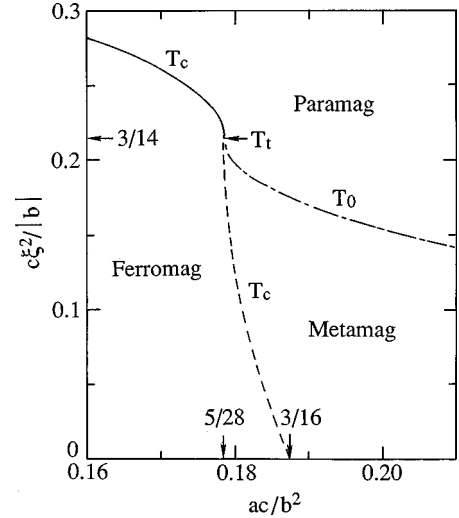


FIG. 15. Theoretical magnetic phase diagram for $a>0$, $b<0$, and $c>0$. The ferromagnetic transition is second order on the solid T_c line ($ac/b^2 < \frac{5}{28}$) and first order on the dotted T_c line ($\frac{5}{28} < ac/b^2 < \frac{3}{16}$). Between the T_c and T_0 lines, the metamagnetic transition occurs. In the narrow region $\frac{5}{28} < ac/b^2 < \frac{3}{16}$, the transition appears just above the first-order T_c line. The T_0 line merges into the T_c line at the point T_t corresponding to $ac/b^2 = \frac{5}{28}$.

tual materials can theoretically be evaluated using the fixed spin-moment method of band calculations.³¹ Hathaway and Cullen³² have actually estimated these coefficients for YCo_2 . At a finite temperature T , the coefficients a , b , and c are renormalized by thermal spin fluctuations and the equation of state is rewritten as

$$B = A(T)M + B(T)M^3 + C(T)M^5, \quad (4)$$

where $A(T)$ is the inverse susceptibility at T . The coefficients $A(T)$, $B(T)$, and $C(T)$ are functions of a , b , c , and the mean-square local amplitude of thermally fluctuating moment $\xi(T)$,² which is proportional to T^2 at low temperatures. In the MY theory, the effects of zero-point spin fluctuations (quantum spin fluctuations) are completely neglected. Moriya²⁴ has determined the magnetic phase diagram of the itinerant electron system with $a>0$, $b<0$, and $c>0$. The negative value of b suggests that the density of states curve has a positive curvature near the Fermi level.¹ In the case of $ac/b^2 > \frac{3}{16}$, the ground state is paramagnetic. The condition for the occurrence of the metamagnetic transition at $T=0$ K is given by

$$a>0, \quad b<0, \quad c>0, \quad \text{and} \quad \frac{3}{16} < \frac{ac}{b^2} < \frac{9}{20}. \quad (5)$$

For $0 \leq ac/b^2 < \frac{3}{16}$, the ground state becomes ferromagnetic. Although the Stoner condition ($a<0$) is not satisfied in this case, ferromagnetism appears. The large positive curvature of the density of states curve near the Fermi level stabilizes the ferromagnetism.

Figure 15 shows the theoretical phase diagram for $a>0$, $b<0$, and $c>0$ in the vicinity of the disappearance of ferromagnetism.²⁴ Because $c\xi(T)^2/|b|$ increases proportionally to T^2 at low temperatures, the ordinate corresponds to the temperature axis of the magnetic phase diagram of

$\text{Co}(\text{S}_{1-x}\text{Se}_x)_2$ indicated in Fig. 8. On the other hand, ac/b^2 increases linearly with x in the narrow region of x and therefore the abscissa is considered as the x axis. The phase transition between the paramagnetic and ferromagnetic states occurs on the T_c line and the metamagnetic transition disappears on the T_0 line. Between the T_0 and T_c lines, the metamagnetic transition appears. With increasing ac/b^2 , the sign of $B(T)$ in Eq. (4) changes from positive to negative on the T_c line and $B(T)$ becomes zero at the critical point T_t where $ac/b^2 = \frac{5}{28}$ is satisfied. Thus, the ferromagnetic transition is second order in the region $0 \leq ac/b^2 < \frac{5}{28}$ and first order in the narrow region $\frac{5}{28} < ac/b^2 < \frac{3}{16}$. The T_t point on the T_c line is considered as the tricritical point where the type of the ferromagnetic transition changes. Moreover, the metamagnetic transition appears just above T_c in the narrow region. The T_0 line merges into the T_c line at T_t . The Curie temperature T_c abruptly decreases with increasing ac/b^2 in the region $\frac{5}{28} < ac/b^2 < \frac{3}{16}$. This phase diagram well reproduces the experimental phase diagram of $\text{Co}(\text{S}_{1-x}\text{Se}_x)_2$ indicated in Fig. 8. CoS_2 with the second-order ferromagnetic transition has no metamagnetic transition above T_c . However, we have found that $\text{Co}(\text{S}_{0.9}\text{Se}_{0.1})_2$ exhibits the first-order ferromagnetic transition and the metamagnetic transition appears above T_c . This dramatic change of the magnetic properties due to the substitution of only 10% Se for S in CoS_2 can be explained by considering that the value of ac/b^2 for CoS_2 is slightly smaller than $\frac{5}{28}$ and increases to a value between $\frac{5}{28}$ and $\frac{3}{16}$ due to the Se substitution. The rapid decrease of T_c in $\text{Co}(\text{S}_{1-x}\text{Se}_x)_2$ and the appearance of the paramagnetic ground state with the metamagnetic transition in magnetic fields can also be explained using the theoretical phase diagram.

According to the MY theory,²⁵ the inverse susceptibility is given by the relation

$$\chi^{-1}(T) = a + \frac{5}{3}b\xi(T)^2 + \frac{35}{9}c\xi(T)^4. \quad (6)$$

This relation indicates that the susceptibility for $a > 0$, $b < 0$, and $c > 0$, and $\frac{5}{28} < ac/b^2 < \frac{9}{20}$ increases and then decreases through a maximum value with increasing temperature.²⁵ Therefore, every paramagnetic system that shows the metamagnetic transition has a broad maximum at a temperature T_{\max} in the temperature dependence of the susceptibility. The itinerant system with the first-order ferromagnetic transition also has a broad maximum in the paramagnetic temperature region. These theoretical results are consistent with the observed magnetic properties of $\text{Co}(\text{S}_{1-x}\text{Se}_x)_2$.

The inverse susceptibility at T_{\max} is written as

$$\chi(T_{\max})^{-1} = \frac{b^2}{c} \left(\frac{ac}{b^2} - \frac{5}{28} \right). \quad (7)$$

The temperature T_{\max} is always higher than T_0 .²⁵ This is consistent with the experimental results of $\text{Co}(\text{S}_{1-x}\text{Se}_x)_2$, as shown in Fig. 8. It should be noted that $\chi(T_{\max})$ becomes infinite at $ac/b^2 = \frac{5}{28}$, where the type of the ferromagnetic transition changes and T_{\max} is equal to the Curie temperature T_c corresponding to the point T_t . (The ferromagnetic region is $0 \leq ac/b^2 < \frac{3}{16}$.) In order to compare the experimental data of $\chi(T_{\max})^{-1}$ with the theoretical relation (7), we have plot-

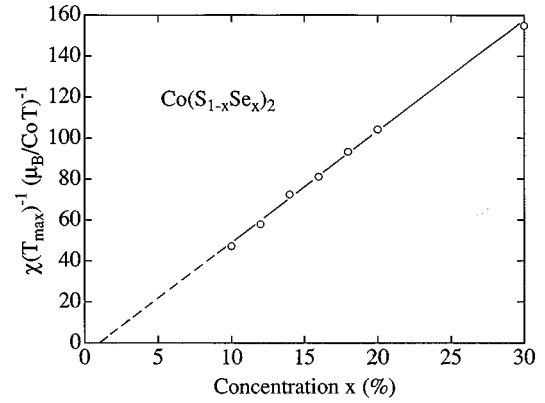


FIG. 16. Inverse susceptibility of $\text{Co}(\text{S}_{1-x}\text{Se}_x)_2$ at $T = T_{\max}$ as a function of the concentration x .

ted the data as a function of x in Fig. 16. These data can well be described by a simple relation,

$$\chi(T_{\max})^{-1} = (540x - 5) [\mu_B/\text{Co}]^{-1}. \quad (8)$$

This relation can be deduced from Eq. (7) and the assumption that the value of a increases linearly with x and those of b and c are nearly constant in the concentration region $0.1 \leq x \leq 0.3$. The susceptibility $\chi(T_{\max})$ becomes infinite at $x = 0.01$. This suggests that the type of the ferromagnetic transition changes at $x = 0.01$. The Curie temperature for $x = 0.01$ corresponds to the point T_t in the phase diagram of $\text{Co}(\text{S}_{1-x}\text{Se}_x)_2$ (see Fig. 8). Therefore, the $\text{Co}(\text{S}_{1-x}\text{Se}_x)_2$ system satisfies $ac/b^2 = \frac{5}{28}$ at $x = 0.01$.

On the other hand, the critical field of the metamagnetic transition near the disappearance of ferromagnetism ($ac/b^2 \cong \frac{3}{16}$) is given by

$$B_c(T) = B_c(0) + \frac{1}{16} \sqrt{|b|/3c} |b| \xi(T)^2, \quad (9)$$

$$B_c(0) = \frac{3}{4} \sqrt{|b|/3c} \frac{b^2}{c} \left[\frac{ac}{b^2} - \frac{3}{16} \right]. \quad (10)$$

[Yamada's expression for $B_c(0)$ includes an error.²⁵] Since the values of b and c of $\text{Co}(\text{S}_{1-x}\text{Se}_x)_2$ will be nearly constant in the narrow concentration region $0.1 \leq x \leq 0.2$, the linear increase of $B_c(0)$ with x mainly comes from the increase of $a = \chi(0)^{-1}$ [see Figs. 6(a), 6(b), and Eq. (1)]. The observed T^2 dependence of $B_c(T)$ originates from the thermal spin fluctuation $\xi(T)^2$ that increases proportionally to T^2 at low temperatures. The fact that α in Eq. (1) does not depend on x indicates that the thermal spin fluctuation in the ferromagnetic compound $\text{Co}(\text{S}_{0.9}\text{Se}_{0.1})_2$ above T_c is equal to that in the paramagnetic compound with $0.12 \leq x \leq 0.2$.

As described above, the magnetic phase diagram of $\text{Co}(\text{S}_{1-x}\text{Se}_x)_2$, the susceptibility $\chi(T_{\max})$ and the critical field $B_c(x, T)$ can qualitatively elucidated with the MY theory. Next, we try to evaluate the parameters a , b , and c and the thermal spin fluctuations $\xi(T)^2$. Since the ferromagnetism of $\text{Co}(\text{S}_{1-x}\text{Se}_x)_2$ disappears at $x = 0.11$, we have $ac/b^2 = \frac{3}{16}$ for $x = 0.11$. We already obtain $ac/b^2 = \frac{5}{28}$ for $x = 0.01$ from Eq. (8). Therefore, we get

$$\frac{ac}{b^2} = 8.93 \times 10^{-2} x + 0.1777. \quad (11)$$

On the other hand, the concentration dependence of the critical field of $\text{Co}(\text{S}_{1-x}\text{Se}_x)_2$ for $T=0$ K, which is shown in Fig. 6(b), is written as

$$B_c(x,0) = 216x - 23.8 \quad [\text{T}]. \quad (12)$$

Using the relations (7), (8), (10), (11), and (12), we can estimate the coefficients a , b , and c within the framework of the MY theory as

$$\begin{aligned} a &= 1.07 \times 10^3 + 5.4 \times 10^2 x \quad [\text{T} (\mu_B/\text{Co})^{-1}], \\ b &= -7.1 \times 10^3 \quad [\text{T} (\mu_B/\text{Co})^{-3}], \\ c &= 8.3 \times 10^3 \quad [\text{T} (\mu_B/\text{Co})^{-5}]. \end{aligned} \quad (13)$$

In the $\text{Co}(\text{S}_{1-x}\text{Se}_x)_2$ system, the second term of Eq. (9) is experimentally expressed as αT^2 with $\alpha = 1.43 \times 10^{-3} [\text{T}/\text{K}^2]$. Using the values of a , b , and c , we obtain the thermal spin fluctuation in $\text{Co}(\text{S}_{1-x}\text{Se}_x)_2$ as

$$\xi(T)^2 = 6.1 \times 10^{-6} T^2 \quad [(\mu_B/\text{Co})^2]. \quad (14)$$

At $T=100$ K, the average local amplitude of the thermally fluctuating moment reaches about $\frac{1}{4} [\mu_B/\text{Co}]$.

The estimated values of a , b , c , and $\xi(T)^2$ can quantitatively explain the experimental values of $\chi(T_{\text{max}})$ and $B_c(x,T)$ and the phase boundaries at $T=0$ K. However, we have found that the value of $\chi(0)$ ($=a^{-1}$) is much smaller than the experimental one. In the case of $\text{Co}(\text{S}_{0.86}\text{Se}_{0.14})_2$, for example, the susceptibility for $T=0$ K is given by $\chi(0) \approx \chi(T_{\text{max}})/16$. As already described, the susceptibility measured at low temperatures is enlarged by the effects of magnetic impurities and sample inhomogeneity. The estimation of the intrinsic value of $\chi(0)$ from the experimental data is difficult. However, the experimental value of $\chi(0)$ in the $\text{Co}(\text{S}_{1-x}\text{Se}_x)_2$ system is obviously much larger than the calculated one. This is because the effect of zero-point spin fluctuations are completely neglected in the MY theory. We consider that the value of $\chi(0)$ obtained from Eq. (13) is close to the one calculated from the density of state at the Fermi level and the Stoner enhancement factor. The susceptibility of $\text{Co}(\text{S}_{1-x}\text{Se}_x)_2$ at $T=0$ K will be enhanced by this effect. Recently, Takahashi and Sakai³³ have proposed a new model that the magnetization process of the itinerant electron system exhibiting the metamagnetic transition is mainly dominated by zero-point spin fluctuations in the ground state.

B. Magnetic properties under static high fields and high pressure

As already described, CoS_2 with the second-order ferromagnetic transition has no metamagnetic transition above T_c , but the application of high pressure $P > 0.4$ GPa changes the ferromagnetic transition into the first-order one. We have observed the metamagnetic transition just above the Curie temperature at $P=0.62$ and 0.77 GPa. These experimental results are summarized in the P - T phase diagram shown in Fig. 11. The pressure dependence of T_c is anomalous above 0.4 GPa: the value of T_c decreases with increasing pressure, but is remarkably higher than that expected from the data below 0.4 GPa. This anomalous change originates from the hysteresis of magnetization due to the first-order ferromag-

netic transition. In the high-pressure experiments, we increased the temperature of CoS_2 after zero-field cooling. Thus, the Curie temperature in the pressure region of the first-order transition is observed to be higher than the equilibrium value of T_c , as seen in the temperature dependence of the magnetization of $\text{Co}(\text{S}_{0.9}\text{Se}_{0.1})_2$ indicated in Fig. 1. We consider that the second-order transition of CoS_2 turns into the first-order one at $P \approx 0.4$ GPa, where the Curie temperature corresponds to the tricritical point T_t . The position of T_c for CoS_2 at 0 GPa exists on the second-order phase boundary near T_t . This phase diagram can also be well reproduced by the theoretical one shown in Fig. 15. Because the application of high pressure increases the value of ac/b^2 and shifts the position of T_c to a point on the first-order phase boundary, the metamagnetic transition appears just above T_c . These facts indicate that CoS_2 is a ferromagnet with a positive value of $a = \chi(0)^{-1}$, which does not satisfy the Stoner condition.

The magnetic properties of ferromagnetic $\text{Co}(\text{S}_{0.9}\text{Se}_{0.1})_2$ with the first-order transition are drastically changed by the application of high pressure. Although the Curie temperature is $T_c = 27$ K at 0 GPa, the ferromagnetism disappears at $P_c = 0.25$ GPa and paramagnetism appears at 0.25 GPa. In the paramagnetic region $P > 0.25$ GPa, the metamagnetic transition takes place even at $T=0$ K. Using the values of T_c and P_c , we can evaluate the pressure dependence of T_c to be $dT_c/dP = -108$ K/GPa. This value is extremely large compared with other itinerant ferromagnets. For example, the value of dT_c/dP is -35 K/GPa for an Invar alloy $\text{Fe}_{64}\text{Ni}_{36}$ with a very large pressure effect of T_c .³⁴ We can easily understand such a large value of dT_c/dP using the theoretical phase diagram. As shown in Fig. 15, the decrease of T_c on the first-order phase boundary with increasing ac/b^2 is very large compared with that on the second-order phase boundary. The critical field of $\text{Co}(\text{S}_{0.9}\text{Se}_{0.1})_2$ as a function of temperature and pressure is given by Eq. (2). The first term is written as

$$B_c(P,0) = 4.25P - 1.06 \quad [\text{T}], \quad (15)$$

where P is expressed in terms of GPa. Equation (15) is very similar to Eq. (12) for the concentration dependence of the critical field at $T=0$ K. This also suggests that both the application of high pressure and the substitution of Se produce almost the same magnetic effects on CoS_2 . Comparing both equations we know that 1% Se substitution corresponds to a pressure of 0.51 GPa. Since the critical concentration x_c of $\text{Co}(\text{S}_{1-x}\text{Se}_x)_2$ is estimated to be $x_c = 0.11$, the ferromagnetism of CoS_2 will disappear at $P_c = 5.6$ GPa.

V. CONCLUSION

CoS_2 is a ferromagnet with the second-order transition at $T_c = 122$ K. The substitution of only 10% Se for S in CoS_2 drastically reduces the Curie temperature to $T_c = 27$ K and the transition becomes first order. $\text{Co}(\text{S}_{1-x}\text{Se}_x)_2$ with $0.12 \leq x$ becomes an exchange-enhanced Pauli paramagnet. The temperature dependence of the susceptibility of ferromagnetic $\text{Co}(\text{S}_{0.9}\text{Se}_{0.1})_2$ shows a broad maximum at a temperature T_{max} in the paramagnetic temperature region, similarly to the paramagnets. We have measured the magnetizations of

$\text{Co}(\text{S}_{1-x}\text{Se}_x)_2$ with $0 \leq x \leq 0.2$ in pulsed high magnetic fields up to 40 T. The itinerant metamagnetic transitions have been observed in the paramagnets. $\text{Co}(\text{S}_{0.9}\text{Se}_{0.1})_2$ also exhibits the transition above T_c . The critical field of the transition increases with increasing temperature as T^2 . Using the experimental data of T_c and the critical temperature T_0 at which the transition disappears, we have determined the magnetic phase diagram in the x - T plane.

We have measured the magnetizations of ferromagnetic CoS_2 and $\text{Co}(\text{S}_{0.9}\text{Se}_{0.1})_2$ under static high magnetic fields and high pressure. With increasing pressure, the Curie temperature of CoS_2 decreases and the second-order ferromagnetic transition changes into the first-order one at $P \approx 0.4$ GPa. In the pressure regime of the first-order transition $P > 0.4$ GPa, we have observed the metamagnetic transition just above T_c . In the case of $\text{Co}(\text{S}_{0.9}\text{Se}_{0.1})_2$, The Curie temperature is drastically decreased by the application of high

pressure and the ferromagnetism disappears at 0.25 GPa. In the paramagnetic pressure region, the clear metamagnetic transition occurs. We have found that the application of high pressure produces almost the same effects on the present system as the Se substitution.

We have analyzed the magnetization data using the MY theory. The observed magnetic properties and the determined magnetic phase diagram of $\text{Co}(\text{S}_{1-x}\text{Se}_x)_2$ can qualitatively be elucidated with this theory. In order to explain these results quantitatively, however, the effects of zero-point spin fluctuations must be included in the theory.

ACKNOWLEDGMENTS

The authors thank H. Yamada for useful discussions. They also thank T. Harada for cooperative research in the early stages of the study.

*Author to whom correspondence should be sent; FAX: +81-3478-5471; Electronic address: goto@mgl.issp.u-tokyo.ac.jp

¹E. P. Wohlfarth and P. Rodes, *Philos. Mag.* **7**, 1817 (1962).

²M. Cyrot and M. Lavagna, *J. Phys. (Paris)* **40**, 763 (1979).

³M. Shimizu, *J. Phys. (Paris)* **43**, 155 (1982).

⁴H. Yamada and M. Shimizu, *J. Phys. F* **15**, L175 (1985).

⁵H. Yamada, T. Tohyama, and M. Shimizu, *J. Magn. Magn. Mater.* **70**, 44 (1987).

⁶D. Bloch, D. M. Zdwars, M. Shimizu, and J. Voiron, *J. Phys. F* **5**, 1217 (1975).

⁷T. Sakakibara, T. Goto, K. Yoshimura, M. Shiga, and Y. Nakamura, *Phys. Lett. A* **117**, 243 (1986).

⁸R. Z. Levitin and A. S. Markosyan, *Sov. Phys. Usp.* **31**, 730 (1988).

⁹T. Goto, K. Fukamichi, T. Sakakibara, and H. Komatsu, *Solid State Commun.* **72**, 945 (1989).

¹⁰T. Goto, T. Sakakibara, K. Murata, H. Komatsu, and K. Fukamichi, *J. Magn. Magn. Mater.* **90/91**, 700 (1990).

¹¹T. Goto, H. Aruga Katori, T. Sakakibara, H. Mitamura, K. Fukamichi, and K. Murata, *J. Appl. Phys.* **76**, 6682 (1994).

¹²T. Sakakibara, T. Goto, K. Yoshimura, and K. Fukamichi, *J. Phys.: Condens. Matter* **2**, 3381 (1990).

¹³M. Iijima, K. Endo, T. Sakakibara, and T. Goto, *J. Phys.: Condens. Matter* **2**, 10 069 (1990).

¹⁴T. Sakakibara, T. Goto, and Y. Nishimura, *J. Phys. Colloq.* **49**, C8-263 (1988).

¹⁵K. Murata, K. Fukamichi, T. Sakakibara, T. Goto, and K. Suzuki, *J. Phys.: Condens. Matter* **5**, 1525 (1993).

¹⁶K. Adachi, M. Matsui, and M. Kawai, *J. Phys. Soc. Jpn.* **46**, 1474 (1979).

¹⁷K. Adachi, M. Matsui, Y. Ohyama, H. Mollmotto, M. Mo-

tokawa, and M. Date, *J. Phys. Soc. Jpn.* **47**, 675 (1979).

¹⁸K. Adachi, K. Sato, and M. Takeda, *J. Phys. Soc. Jpn.* **26**, 631 (1969).

¹⁹T. A. Bither, R. J. Bouchard, W. H. Cloud, P. C. Donohue, and W. H. Siemons, *Inorg. Chem.* **7**, 2208 (1968).

²⁰H. S. Jarret, W. H. Cloud, R. J. Bouchard, S. R. Butler, C. G. Frederick, and J. L. Gillson, *Phys. Rev. Lett.* **26**, 617 (1968).

²¹A. Ohsawa, H. Yamamoto, and H. Watanabe, *J. Phys. Soc. Jpn.* **37**, 568 (1974).

²²W. Folkerts, G. A. Sawatzky, C. Haas, R. A. de Groot, and F. U. Hillebrecht, *J. Phys. C* **20**, 4135 (1987).

²³H. Yamada (private communication).

²⁴T. Moriya, *J. Phys. Soc. Jpn.* **55**, 357 (1986).

²⁵H. Yamada, *Phys. Rev. B* **47**, 11 211 (1993).

²⁶H. Yasuoka, N. Inoue, M. Matsui, and K. Adachi, *J. Phys. Soc. Jpn.* **46**, 689 (1979).

²⁷G. Krill, P. Panissord, and M. F. Lapiere-Ravert, *J. Phys. C* **12**, 4269 (1979).

²⁸T. F. Smith and C. W. Chu, *Phys. Rev.* **159**, 353 (1967).

²⁹K. Murata, K. Fukamichi, T. Sakakibara, T. Goto, and H. Aruga Katori, *J. Phys.: Condens. Matter* **5**, 2583 (1993).

³⁰S. Yomo, *J. Phys. Soc. Jpn.* **47**, 1486 (1979).

³¹V. L. Moruzzy, P. W. Murcus, K. Schwarts, and P. Mohn, *Phys. Rev. B* **34**, 1784 (1986).

³²K. Hathaway and J. Cullen, *J. Phys.: Condens. Matter* **3**, 8911 (1991).

³³Y. Takahashi and T. Sakai, *J. Phys.: Condens. Matter* **7**, 6279 (1995).

³⁴J. M. Leger, C. Loriers-Susse, and B. Vodar, *Phys. Rev. B* **6**, 6 (1972).